Relationship between soil water content and soil particle size on typical slopes of the Loess Plateau during a drought year

Xiao Zhang [a,b,c], Wenwu Zhao [a,b,*], Lixin Wang[c], Yuanxin Liu [a,d], Yue Liu [a,b], Qiang Feng [a, e]

a. State Key Laboratory of Earth Surface Processes and Resource Ecology, Faculty of Geographical Science, Beijing Normal University, Beijing 100875, China;
E-Mails: zhangxiao9005@gmail.com (X. Z.); yuanxinliu@rcees.ac.cn (Yuanxin L.); 201531190025@mail.bnu.edu.cn (Yue L.); 201231190029@mail.bnu.edu.cn (Q. F.)

b. Institute of Land Surface System and Sustainable Development, Faculty of Geographical Science, Beijing Normal University, Beijing 100875, China

c. Department of Earth Sciences, Indiana University–Purdue University Indianapolis (IUPUI), Indianapolis, Indiana 46202, USA; lxwang@iupui.edu (L. W.)

d. State Key Laboratory of Urban and Regional Ecology, Research Center for Eco-Environmental Sciences, Chinese Academy of Sciences, Beijing 100085, China.

e. College of Forestry, Shanxi Agricultural University, Taigu, Shanxi 030801, China

***** corresponding authors:
Zhao Wenwu, E-Mail: zhaoww@bnu.edu.cn
Tel.: +86-10-58802125; Fax: +86-10-58802125.

This is the author's manuscript of the article published in final edited form as:

Zhang, X., Zhao, W., Wang, L., Liu, Y., Liu, Y., & Feng, Q. (2019). Relationship between soil water content and soil particle size on typical slopes of the Loess Plateau during a drought year. Science of The Total Environment, 648, 943-954. https://doi.org/10.1016/j.scitotenv.2018.08.211

Abstract

In the context of global climate change as well as local climate warming and drying on the Loess Plateau of China, understanding the relationship between soil particle size and soil water distribution during years of atypical precipitation is important. In this study, fractal geometry theory is used to describe the mechanical composition and texture of soils to improve our understanding of hydropedology and ecohydrology in the critical zone on the Loess Plateau. One grassland slope and two shrubland slopes were selected in the hilly and gully region of the Loess Plateau, and soils were sampled along hillslope transects at depths of 0-500 cm. Fractal theory and redundancy analysis (RDA) were used to identify relationships between the fractal dimension of soil particle-size distributions and the corresponding van Genuchten parameters for the soil-water-characteristic curves. The oven-drying method was used to measure soil water content, and the high-speed centrifugation method was used to generate soil-water-characteristic curves. The results show that (1) the soil water that can be used by *Caragana korshinskii* during a drought year is distributed below 2 m from the surface, whereas the soil water that can be used by grass is below 1.2 m; (2) *Caragana korshinskii* promotes the conservation of fine soil particles more than does natural restored grass, and the soil particle-size distribution fractal dimension changes with depth and position; and (3) soil hydraulic properties correlate strongly with soil pedological properties such as bulk density and the soil particle-size distribution fractal dimension. These results provide a case study of the relationships among soil distributions, hydrologic and geomorphic processes for vegetation restoration in drylands with a thick vadose zone. More studies on soil property changes are needed to provide case studies and empirical support for ecological restoration in the Loess Plateau of China.

Keywords: particle-size distribution; soil-water characteristic curve; fractal dimension; drought year; Loess Plateau

1. Introduction

The Loess Plateau of China is a critical area because it occupies a large areas of arid and semiarid areas and feeds a large amount of the country's population; however, the ecosystem is fragile, and the loose soil is easily eroded (Fu et al., 2002; Lü et al., 2012). With global climate change, extreme weather events have increased, and the climate of the Loess Plateau has become drier and warmer. These changes threaten local ecological restoration (Qin et al., 2002, 2014; Stocker et al., 2013). To conserve soil and water and to control desertification of the Loess Plateau, the Chinese government conducted the *Grain to Green* program in 1999. As the area and age of the shrub- and grass-planting areas have increased, the conflict between water consumption by different types of vegetation planted and soil desiccation has become more evident (Lü et al., 2012; Wang et al., 2004, 2010, 2011). The loess hilly and gully region is the key area of soil and water conservation in the Loess Plateau and is home to millions of people (Fu et al., 2002; Wang and Shao, 2000). The soil in this area is loose with strong erodibility, and the landscape is the most fragmented and rugged of

all of the areas in the Loess Plateau. The average amount of soil erosion in this region is more than 2000 t/(km^{2}yr) and is even over 20000 t/(km^{2}yr) in the worst areas (Fu, 1989; Shi and Shao, 2000). The precipitation is concentrated in the summer and most of the intensity of the rainfall is strong and erosive. In this region, grasses and shrubs are the most common vegetation types, occupying more than half of the total area (Zhao and Running, 2010). Most commonly, the dominant species of natural restored grassland (from abandoned slope farmland) are forage grasses, and artificial shrubland restoration uses *Caragana korshinskii* (Wang et al., 2009b; Yao et al., 2012). Precipitation is the only source of soil water that can be used by plants in this area (Jiao et al., 2006; Ning et al., 2013; Yan et al., 2015; Yu et al., 2015b). Due to the close relationship between plant growth and soil water content (Wang et al. 2012), studies of soil water under typical vegetation types in this region have changed from focusing on water content to water movement and hydraulic characteristics (Lü et al., 2014a; Shao et al., 2006). Soil available water is the water that can be directly used by plants and is therefore a more useful indicator than volumetric water content, particularly in the context of vegetation growth (Fang et al., 2016; Gao et al., 2015; Wang et al., 2013). Soil available water greatly depends on soil texture and structure (Shao et al., 2006). Soil water content is unable to reach field capacity in the semi-arid Loess Plateau because the amount of evapotranspiration is larger than that of precipitation and the loose soil and deep ground water causes soil moisture infiltration into the deep layer. Texture is an important aspect of soil morphology that can impact the ability of the soil to conserve water as well as support root growth, and strongly influences soil hydraulic characteristics and erosion (Gui et al., 2010; Li et al., 2016; Meskini-Vishkaee et al., 2014; Nguyen et al., 2013). Research on the changes in soil water content and soil texture under different land-use types may reveal the relationships between these factors and long-term vegetation restoration in this erodible area.

The soil-water characteristic curve is important for estimating soil hydraulic parameters that are difficult to measure in the field, such as the wilting point. New techniques require specialized equipment, and the acquisition of undisturbed soil samples from deeper soil layers remains difficult on the Loess Plateau (Arya and Paris, 1981; Daly et al., 2015; Nimmo et al., 1987; Nimmo and Mello, 1991). To solve these issues, the estimation of soil hydraulic properties through inverse modeling has become popular, but it is also time- and resource-consuming (Hopmans and Simunek, 1999; Mirus et al., 2009; Vrugt et al., 2008). Many studies have focused on predicting parameters that are difficult to measure directly based on more easily quantifiable parameters (Carsel and Parrish, 1988; Meskini-Vishkaee et al., 2014; Schaap et al., 2001; Vereecken et al., 2010). The models used to generate soil-water characteristic curves can be divided into direct-fitting (Brooks and Corey, 1964; Campbell, 1974; van Genuchten, 1980) and indirect-calculation methods (Arya and Paris, 1981; Liu and Xu, 2003; Peng et al., 2014). Among the direct-fitting models, the van Genuchten model has been shown to provide good results for most soils in the loess hilly and gully regions of Loess Plateau (Lai and Wang, 2003; Wang et al., 2009a). Since the concept of fractal dimensions has been introduced to soil science

with the development of the laser diffraction technique, soil fractal dimensions have received increasing attention (Kong and Song, 2015; Li et al., 2016; Peng et al., 2015). The volume-based fractal model has been proven to be ideal for evaluating and describing soil hydraulic properties as well as soil physical properties and potential (Jin et al., 2013; Montero, 2005; Posadas et al., 2001; Wang et al., 2011; Yang et al., 2008; Yu et al., 2015a).

Most of the research on the relationship between grass- and shrubland ecosystems at the plot and slope scales has been undertaken during normal years, whereas fewer studies have been conducted during drought years (Liu et al., 2007; Liu et al., 2016b; Wang et al., 2014; Yang et al., 2014a; Zhang et al., 2016a). Due to the stronger evapotranspiration on south-facing slopes, the soil water contents on such slopes are markedly lower than those on north-facing slopes; thus, south-facing slopes are more prone to water deficiency under the same precipitation conditions. In this context, studies of the soil water conditions and soil properties of south-facing slopes under different vegetation types during drought years can provide reference baselines for restoration under future climate change scenarios (Lü et al., 2015; Qiu et al., 2001). In this study, two shrubland slopes dominated by *Caragana korshinskii* and one grassland slope dominated by forage grasses, all of which are south-facing slopes, were chosen as study locations. The soil water content, soil-water characteristic curve, soil available water, soil particle-size distribution, and singular and multiple fractal dimensions of soil particle size were measured or calculated at different positions and depths along the slopes. This study aimed to (1) analyze the distribution of soil water content, soil particle size and relevant parameters along typical slopes of the Loess Plateau in a drought year and (2) analyze the relationship between soil particle dimension and the soil available water content to provide a case study of a semi-arid loess area for vegetation restoration management. The hypotheses of this study were as follows: (1) There are significant differences in the depth of water use between grassland and shrubland in a drought year and (2) the relationship between soil particle fractal dimension and the soil-water characteristic curve varies between types of vegetation restoration and among slope positions and soil layer depths.

2. Materials and methods

2.1 Site description

This study was conducted in Liuping Gully in the Ansai Catchment, Shaanxi, China, which is located along the upper reaches of the Yanhe River and belongs to the typical loess hilly gully region of the Loess Plateau. The longitude and latitude are 108°5’-109°26’E, 36°19’-36°32’N, and the area of the Liuping watershed is 24.26 km^2. The landscape is fragmented, and the gully density is high. The study site is located in a temperate semi-arid continental climate zone, and the spatial and temporal distributions of the precipitation are uneven both intra- and inter-annually. The precipitation is concentrated in the summer; rainfall from June to September contributes more than 60% of the annual precipitation. The thickness of loess soil is 50-200 m on

the Loess Plateau, and the water table is very deep (usually 30 m to 80 m from the surface soil layer and participating little in soil-vegetation-atmosphere-transfer) (Shao et al., 2015), making the groundwater almost inaccessible to plants. The soil is porous, and the heavy rain in the summer makes the soil prone to erosion.

Three slopes in the Liuping Gully that are typical of shrub and grass slopes in the loess hilly and gully region were chosen for study. The dominant species on slopes 1 and 2 is *Caragana korshinskii*, and the dominant species on slope 3 are *Bothriochloa ischaemum, Stipa grandis,* and *Stipa bungeana.* The soil type on all slopes is mainly loessial, and the elevation ranges from 1,190 m to 1,335 m. The sampling year (2015) was a drought year with a total rainfall of 393 mm, which is 13.7-21.4% less than the multiyear mean precipitation of approximately 450-500 mm (Chen et al., 2008; Zhang et al., 2016). The sampling lasted four days, during which no rain occurred, and the last rain came six days before sampling with an amount of 0.2 mm, which had little impact on the soil water conditions. Therefore, the variation in the soil water content was not affected by precipitation during sampling. Due to the reduced rainfall in drought years, the water content in the shallow soil layers (0-2 m) was very low while that in deep layers was temporally stable; therefore, evaporation had little influence during the sampling period.

2.2 Experimental design

Using Google Earth images, slopes with large areas of shrub or grass were preselected for field study. The reachability, length, vegetation type, vegetation coverage, and vegetation restoration age of the preselected slopes were investigated during a trip to the field. Two shrubland slopes and one grassland slope in Liuping Gully were chosen from the preselected slopes as they are typical in the research area. In addition, the two kinds of slopes are close to one another, which avoids the influence of precipitation or other environmental factors in the analysis. Nine sampling points were established from the foot to the top of each slope. In this study, CK denotes for *Caragana korshinskii* shrubland, and NG denotes for natural restored grassland. On slope 1, the sampling points were numbered CK1 to CK9 from the bottom of the slope to the top; on slope 2, the sampling points were numbered CK10 to CK18, and from NG1 to NG 9 on slope 3 (Figure 1). The distribution of the dominant species in the two shrub slopes was uniform. On the grass slopes, although the dominant species were Gramineae species, the distribution of individual species was more heterogeneous than that one the shrub slopes. Therefore, the sampling interval on the shrub slopes was greater than that on the grass slopes ensuring more representative sampling. Based on the actual length of the slope, the final distance between two adjacent sampling points was 20 m on the slopes with shrubs and 15 m on the grassland slope.

[please insert Figure 1 here]

Figure 1 Study area location map and photograph illustrating the distribution of soil sampling points. Notes: CK represents *Caragana korshinskii* shrubland, and NG represents natural restored grassland.

The deepest sampling depth was 5 m because the effect of artificial vegetation on soil moisture is deep in the Loess Plateau and the root system range of most plants is generally concentrated at a depth of 0-5 m (Fang

et al., 2016; Yang et al., 2014b). Samples were collected at 20-cm intervals between 0 and 1 m and at 100-cm intervals between 1 and 5 m. Three replicates per sampling point were collected using a soil auger with a 5-cm diameter, and each sample was divided into two parts. One part was placed in an aluminum box to measure the soil water content using the drying method at 105°C, and the other part was used to determine soil particle size using a Mastersizer 2000 (Malvern Instruments Ltd., Worcestershire, United Kingdom) after removal of the organic matter and dispersion with H_2O_2 (10%), HCl (10%) and SHMP (sodium hexametaphosphate).

Undisturbed soil samples were collected on slopes 2 and 3 by excavating the soil profiles and using cutting rings at the top of the slope, the middle of the slope and the bottom of the slope. Samples were collected from four depth layers: 0-40 cm, 40-80 cm, 80-120 cm and 120-200 cm. Two cutting rings with different volumes were used simultaneously, and there were three replicates at each point. Soil samples collected with the 100-cm^3 cutting rings were used to determine bulk density with the drying method, and samples collected with the 200-cm^3 cutting rings were transferred into centrifuge tubes to determine the soil-water characteristic curves using a high-speed refrigerated centrifuge (CR2G, Hitachi Ltd., Tokyo, Japan) (Khanzode et al., 2002; Reatto et al., 2008). When the centrifugal force came to 1.5 MPa, the soil water content under this pressure is considered as the wilting point in the analysis (Shao et al., 2006).

The aboveground biomass was determined at the top, middle and bottom of each slope, and three replicated sampling plots were established at each position. The area of the plots was 5 × 5 m on the slopes with shrubs (slope 1 and slope 2) and 2 × 2 m on the slope with grass (slope 3). Plant samples were collected using the cutting method from 5 small subplots with a dimension of 20 × 20 cm that were randomly distributed in each plot and dried to a constant weight at 75°C.

2.3 Data analysis

2.3.1 Fitting of the soil-water characteristic curve

The soil-water characteristic curve was fitted using the van Genuchten model (van Genuchten, 1980) according to Equation (1), and the soil volumetric water content (cm^3/cm^3) was converted to soil mass water content (g/g) using Equation (2):

$$\frac{\theta-\theta_r}{\theta_s-\theta_r}=\left(\frac{1}{1+(\alpha\times h)^n}\right)^m \quad , \tag{1}$$

$$\theta=\theta_m\times\frac{BD}{\rho_w} \quad , \tag{2}$$

where θ represents the soil volumetric water content (cm^3/cm^3); θ_m represents the soil mass water content (g/g); h represents the pressure head (cm); ρ_w represents the water density (ρ_w = 1.0 g/ cm^3 in this study); θ_s and θ_r, represent the saturated and residual water content values, respectively, which were calculated from existing data; α, n and m are empirical parameters (m = 1-1/n in this study) that also must be calculated from existing

data (or termed model coefficients); and BD represents the soil bulk density.

2.3.2 Fractal analysis of soil particle-size distribution

The size of the soil particles was divided into clay (< 2 μm), silt (2-50 μm) and sand (50-2000 μm) according to the USDA (United States Department of Agriculture) classification. Almost all of the soil samples were characterized as silt loam, and soil particles between 3.95-106.637 μm in size were represented in more than 80% of samples (Figure 2, Supplementary 1). Using a combination of data from this study and standard practices from previous studies (Song and Li, 2011; Wang et al., 2007), soil particle sizes between 0.03-2000 μm were divided into 64 levels according to the logarithmic interval in the singular fractal analysis, while soil particle sizes between 0.3-1500 μm were divided into 64 levels according to the logarithmic interval in the multifractal analysis.

[please insert Figure 2 here]

Figure 2 Texture of the studied soil samples. Note: CK represents the soil under *Caragana korshinskii* Kom, and NG represents the soil under natural restored grassland.

The singular fractal dimension (F) of the soil particle-size distribution was calculated using Equation (3). Logarithms were taken on both sides of Equation (3) to obtain Equation (4), and (3 - F) represents the slope of the logarithmic linear regression equation:

$$\frac{v\left(r<R_i\right)}{V_r}=\left(\frac{R_i}{R_{\max}}\right)^{3-F} \quad , \qquad (3)$$

$$\log\left(\frac{v\left(r<R_i\right)}{V_r}\right)=\left(3-F\right)\log\left(\frac{R_i}{R_{\max}}\right) \quad , \qquad (4)$$

where $v\ (r < R_i)$ represents the cumulative percentage of particles with a radius less than R_i (mm); V_r represents the total percentage of particles (V_r = 100); R_i represents the particle radius (mm) of the i size class; and R_{max} represents the largest particle class radius (R_{max} = 2 mm in this study).

The multifractal dimension (Peitgen et al., 1992), which is also known as the Rényi dimension (Montero, 2005), of the soil particle-size distribution was calculated using Equation (5) ($q \neq 1$) and Equation (6) (q = 1).

$$D_q=\frac{1}{q-1}\lim_{\varepsilon\to 0}\frac{\sum_{i=1}^{N_{(\varepsilon)}}\mu_i\left(\varepsilon\right)^q}{\log\left(\varepsilon\right)} \quad (q\neq 1) \quad , \qquad (5)$$

$$D_1=\lim_{\varepsilon\to 0}\frac{\sum_{i=1}^{N(\varepsilon)}\mu_i\left(\varepsilon\right)\log\mu_i\left(\varepsilon\right)}{\log\left(\varepsilon\right)} \quad (q=1) \quad , \qquad (6)$$

where q represents the moment order of the distribution (q ranged from -10 to 10 with a 0.5 step interval in this study); $N(\varepsilon)$ represents the number of cells needed to cover the entire interval; ε represents the cell sizes; and $\mu(\varepsilon)$ represents the mass of the soil particles in this subinterval. When q = 0, the D_0 is called the capacity

dimension (or the box-counting dimension), which accounts for the scaling properties and average information of a system, and it represents the dimension of the sizes that were set using a nonzero relative volume (the cell) (Montero, 2005; Posadas et al., 2001; Voss, 1988). When $q = 1$, D_1 is known as the entropy dimension, which shows the scaling in the concentration of the parameter with cell interval and is related to the information or Shannon entropy (Andraud et al., 1994, 1997; Montero, 2005; Posadas et al., 2001; Shannon, 2001). When $q = 2$, D_2 is known as the correlation dimension and is mathematically associated with the correlation function. When the fractal is statistically or exactly self-similar and homogeneous, the equality $D_0 = D_1 = D_2$ occurs (Gouyet, 1996; Grout et al., 1998; Posadas et al., 2001).

2.3.3 Statistical analysis

Variations in the physical properties and water content of the soil at different slope positions and soil depths were analyzed by one-way analysis of variance (ANOVA), and the least squares difference method (LSDM) was utilized to verify the results. Correlations between the soil water content and the influencing factors were verified with Pearson's contingency coefficient (2-tailed; significant at $P < 0.05$; very significant at $P < 0.01$). After performing detrended correspondence analysis (DCA), the lengths of the gradient of the first axis were found to be shorter than 3.0; therefore, linear constraint-sorting redundancy analysis (RDA) was chosen to evaluate the correlations between each of the soil physical properties and water contents.

3. Results

3.1 Soil water content distribution and soil water-characteristic curve

The soil water content was constant at a lower level between 0 and 500 cm on the shrubland slopes (slopes 1 and 2) and between 0 and 100 cm on the grassland slope (slope 3), and soil water content increased with increasing soil depth. The difference in water content from the bottom of the slope to the top of the slope was not significant in the shallow layers, but the water content generally decreased from the bottom of the slope to the top of the slope in the 2-5-m layer. The soil water content at a depth of 0-100 cm was lower than that at 200-500 cm (LSDM, 0.05) on all slopes. The mean soil water content on the grassland slope was higher than that on the shrubland slopes at a depth of 0-500 cm, while the mean value on the grassland slope was lower than that on the shrubland slopes at a depth of 0-100 cm (Figure 3).

[please insert Figure 3 here]

Figure 3 Distribution of the soil water content at different depths (a) and different positions along the slopes (b).

Soil particle sizes were calculated, and the results are shown in Table 1. *D[3,2]* indicates the average particle size of a specific surface area, and *D[4,3]* indicates the average particle size of a volume surface area. The value of *R* (which equals *D[3,2]/D[4,3]* in this paper) was close to 1 when the shape of the particles became increasingly regular and the soil particle-size distribution became more centralized. In Table 1, d(0.1) indicates that soil particles of this size constitute 10% of all soil particles, d(0.5) indicates that soil particles of this size constitute 50% of all soil particles and d(0.9) indicates that soil particles of this size constitute 90% of

all soil particles. The d(0.1), d(0.5), d0.9, *R*, and sand content values increased from the bottom of the slopes to the top, and the differences among the different positions were significant (LSDM, 0.05). The mean soil water content at the bottoms of the slopes was higher than that in the middle and at the top. According to a comprehensive analysis of *R*, d(0.5) and soil water content, particles in the lower slope position had a more regular shape and were smaller in average size than those in the upper slope position, while the soil water content in the lower slope position was higher than that in the upper slope position (Table 1).

[please insert Table 1 here]

Soil-water characteristic curves were fitted using centrifugation data and Equations (1) and (2). The results are shown in Figure 4 and Table 2 and indicate that the van Genuchten model fits the sample data well. The wilting points on the slopes ranged from 0.52 g/g to 0.87 g/g, and the soil water content ranged from 0.24 g/g to 0.87 g/g. The wilting point on the shrubland slope (slope 2) was higher than on the grassland slope (slope 3), while the soil water content on the shrubland slope was lower than on the grassland slope. On the shrubland slope, the soil water contents were lower than the wilting points in all soil layers, and on the grassland slope, the soil water contents were lower than the wilting points at depths between 0-120 cm.

[please insert Figure 4 here]

Figure 4 Soil-water characteristic curves at different slope positions and soil depths.

[please insert Table 2 here]

3.2 Distributions of singular and multiple fractal dimensions on the slopes

The singular and multiple fractal dimensions were calculated using soil particle-size data and Equations (3), (4), (5) and (6), and the results are shown in Figure 5 and Figure 6. Figure 5 shows that the logarithmic coordinates of the singular fractal dimension for each sample can form a line and that the lines for all the samples have two inflection points. The inflection points are close to the points that separate the soil into clay, silt and sand according to the Kaczynski classification system (0-1 μm, 1-50 μm, and 50-2000 μm, respectively); therefore, the lines are divided into three sections (the sand domain, the silt domain, and the clay domain) with significantly different slopes. The value of the singular fractal dimension (*F*) equals 3 minus the slope of the logarithmic linear regression line, and the *F* values are significantly different among these three domains. Overall, the singular fractal dimensions at different depths were more dissimilar on the grassland slope (slope 3) than on the other two slopes and were more dissimilar at the top of the slope than at the other positions. Figure 6 shows the summary spectra of the multifractal dimensions at different positions and depths. In the Rényi dimension, $D_{(q)}$ decreased with increasing q. D_0 (box dimension) provides the basic soil particle size information, and it ranges from 0 to 1 as the soil particle size distribution becomes broader. D_1 (entropy dimension) provides a tool to describe the heterogeneity in soil particle size, and it increases with increasing heterogeneity. The combined index, D_1/D_0, better reflects soil particle size heterogeneity (Posadas et al., 2001), and D_2 (correlation dimension) also reflects the degree of uniformity.

[please insert Figure 5 here]

Figure 5 Log-log plots of soil particle size distributions for samples at different depths and slope positions.

[please insert Figure 6 here]

Figure 6 Multifractal Rényi spectra *Dq*-q curves of soil samples from different depths and slope positions.

The mean values of the singular and multiple fractal dimensions at various slope positions and soil depths are shown in Supplementary 2 and 3. Supplementary 2 shows that the singular fractal dimensions on the shrubland slopes increased from the top of the slope to the bottom, while the singular fractal dimension on the grassland slope changed irregularly. D_0 and D_1 first increased and then decreased from the top of the slope to the bottom, and *Fsilt* increased from the top to the bottom on the two shrubland slopes (slopes 1 and 2); however, the changes were not significant (LSDM, 0.05). Supplementary 3 shows that the mean values of D_1/D_0 on the two shrubland slopes (slopes 1 and 2) were lower than on the grassland slope (slope 3), but no differences in D_2 among these slopes were evident (Supplementary 2). Both the soil water content and the singular fractal dimensions first increased and then remained relatively stable as soil depth increased, and D_0 decreased and then remained relatively constant with increasing depth. D_1 and D_2 were higher at depths between 0-40 cm, below which they were lower and changed irregularly. D_1/D_0 in the 20-200-cm soil layers was lower than in the 300-500 cm layers (Supplementary 3).

3.3 Factors influencing soil water content and wilting point

Using the soil particle size, the soil water content data and the soil-water characteristic curves, the correlations between the soil water content and the factors *R*, sand content, silt content, clay content, *F*, *Fsand*, *Fsilt*, *Fclay*, D_0, D_1, D_2, bulk density, biomass, slope, and position were subjected to a 2-tailed test using Pearson's contingency coefficient (Supplementary 4). The species data were verified using a detrended correspondence analysis (DCA) (length of gradient < 3), and the data gradient (Figure 7) was then determined from the RDA of the soil water content at different depths and other factors described in Supplementary 4. Supplementary 4 and Figure 7(b) show that the soil water content was significantly positively correlated with silt content, clay content, *F* and depth, while it was significantly negatively correlated with sand content. The wilting point was significantly positively correlated with silt content, clay content, depth and biomass, while it was significantly negatively correlated with sand content. Among the other factors, D_0, D_1 and D_2 all had significant negative correlations with bulk density, while *R* had a significant positive correlation. The values of D_0 and D_1 increased with increasing sand content and decreasing in silt content and *R*. *R* was significantly positively correlated with silt content (Supplementary 4, Figure 7).

The relationships between soil water content and the relevant factors at different depths are shown in Figure 7(a). The soil water content had a positive correlation with silt content, clay content, F_{sand} and *F* in the 0-100 cm soil layers, and it had a positive correlation with position, D_1, D_2, D_{silt} and slope in the 200-500 cm soil layers. The soil water content was negatively correlated with sand content in the 0-100 cm soil layers and

with *R* in the 200-500 cm soil layers. Biomass exhibited a positive correlation with soil water content in the 0-100 cm soil layers, but the relationship was negative in the 200-500 cm soil layers (Figure 7).

[please insert Figure 7 here]

Figure 7 Relationships between soil water content and the relevant factors (a) at different depths, as well as the relationships between soil water indices (soil water content and wilting point) and the relevant factors (b).

Note: Sand% represents sand content; silt% represents silt content; clay% represents clay content; Fsa represents *Fsand*; Fsilt represents *Fsilt*; Fcl represents *Fclay*; BIO represents biomass; R represents *D[3,2]/D[3,4]*; SWC represents soil water content; wp represents the wilting point; and the numbers 20, 40, 60, 80, 100, 200, 300, 400, 500, etc. in the left figure (a) represent the soil layer depth (cm).

4. Discussion

4.1 Spatial variation in soil water and wilting point at the transect scale

There is a long history of soil water content research on the Loess Plateau. After many years of vegetation restoration, the soil water conditions have changed considerably. A previous study in a normal year (Fang et al., 2016) and our study in a drought year (Figure 3) have both shown that the soil water content is lower under CK than under NG.

At various depths, the differences in soil water content between shrubland and grassland increased from the top layer to the deeper layers of the soil profile, and the average soil water content was higher in the shallow layers (0-2 m) than in the deep layers (2-5 m) in normal years (Liu et al., 2016b; Zhang et al., 2016). During a drought year, the shallow soil layers receive little rainfall, and evapotranspiration and root uptake resulted in less soil water content in the 0-2 m soil layers than in the 2-5 m layers (Figure 3).

At various slope positions, from top to bottom of the slope, the soil water content typically increased, but this relationship can change as the slope increases (Gao et al., 2011; Huang et al., 2013). In this study, the soil water content decreased inconsistently from the bottom of the slope to the top and remained low at all positions, but the degree of change was smaller in the shallow layers (0-2 m) than in the deep layers (2-5 m) in the drought year (Figure 3, Table 1). This may imply that it is difficult for water loss to continue due to the lower soil water content in the shallow layers; CK seemed to use less water from the shallow soil layers (0-1 m) under drought conditions. In deep soil layers below 2 m, the increase in amplitude was higher in NG than in CK during a drought year (Figure 3) and was similar to that of normal years (Zhang et al., 2016). The variation in soil available water content and the variation in soil water content were similar to each other along the slopes. Soil water content at the depth of 0-2 m under CK and at 0-1.2 m under NG was lower than the wilting point. The only available soil water that could be used by CK was below 2 m, but the soil water that could be used by grass was below 1.2 m during the summer in a drought year (Table 2). As dry years might occur more frequently in the future, introduced shrubs such as *Caragana korshinskii* would have a negative effect on vegetation restoration in drylands with thick soil layers and deep ground water.

4.2 Spatial variation in the soil particle size distribution at the transect scale

The soil particle-size distribution has been found to be essential to the formation of soil structure and soil nutrient conservation (Jiménez et al., 2008; Liu et al., 2016a; Marques et al., 2015; Peng et al., 2015; Song et al., 2015; Sun et al., 2016a; Yu et al., 2015a). Fine particles smaller than 50 μm (clay and silt) retain soil organic carbon better than coarse sand; therefore, nutrient and soil organic carbon losses mainly occur because of the loss of clay and silt from soils (Jin et al., 2013; Wang et al., 2007; Zhao et al., 2014). In this study, fine particles increased and coarse particles decreased from the top of the slope to the bottom of the slope (Table 1). Therefore, the shape of the soil particles became more uniform, and d(0.5) increased while the water-holding capacity decreased from the bottom of the slope to the top (Table 1). When water flows from the top of the slope to the bottom of the slope under a normal erosion process, fine particles are removed first as they are more easily eroded than coarser particles, and during this movement, these particles become ball-shaped as their surfaces are smoothed (Table 1). As more fine particles move to the lower position of the slope, the average soil particle size is smaller than that in the upper slope (Supplementary 1 and Table 1). Existing studies have shown that different kinds of plants might have different influences on soil texture and properties (Cortina and Maestre, 2005; Gu and Luo, 2016; Li et al., 2012). For example, the conversion from cropland to other types of vegetation in the Loess Plateau was more effective for improving soil conditions in deep soil layers (Sun et al. 2016b), while studies in the northern part of the Loess Plateau showed that conversion from cropland to shrub or grass land worsened water conditions in the deep soil profile (Zhang et al. 2018). In this study, more fine particles were found in shrublands than grasslands, indicating that shrublands were more efficient at trapping the fine sediments, protecting fine soil particles better than grasses (Supplementary 1).

The values of F_{clay} were found to be lower than 0 in previous studies (Wang et al., 2007) as well as in this study (Supplementary 2), which means that the data from the laser particle-size analysis are not very accurate for the clay domain. However, analyses of other domains have proven to be useful in discussing the soil particle distribution and fractal dimensions (Bai and Wang, 2012; Dong and Zheng, 2010; Ru et al., 2015). Existing studies show that indices such as F, F_{silt}, F_{sand}, D_0, D_1, D_2 and D_1/D_0 highly correlate with soil organic matter, and these measures can potentially be used to reflect soil quality (Marinho et al., 2017; Wang et al., 2007; Zaffar and Lu, 2015; Zhang et al., 2012a, 2012b). These indices also differed at different slope positions and soil depths in this study. As the depth increased, the soil water content, F, and F_{sand} increased, while D_0 decreased (Supplementary 3). The D_1 and D_2 values in the 0-40-cm soil layers were higher than in the 60-500-cm soil layers, which means that there were more differences among the soil particles in shallow layers than among those in deep layers (Supplementary 3). As fine particles are more easily removed by runoff or soil water movement than are coarse particles, the range of the soil particle-size distribution was larger at the bottom of the slope than at the top on the two shrub slopes (Table 1 and Supplementary 2), whereas on the grass slope, the F, D_0, D_1 and D_2 values at the middle position were lower than those at the other positions

(Supplementary 2). These changes occurred not only on the soil surface but also in the different soil layers (Figure 6 and Supplementary 3). Therefore, CK should be planted lower on the slope, and NG should be restored in the upper slope position to maintain the sustainability of vegetation restoration in this area.

4.3 Correlations between soil particle size and soil hydraulic parameters

Soil physical, pedological and hydrological properties are intrinsically connected (Lin, 2010; Montenegro and Ragab, 2012; Venkatesh et al., 2011; Vivoni, 2012; Yao et al., 2012; Zhao et al., 2011). The wilting point obtained from the soil-water characteristic curve showed significant correlations with F, clay content, silt content and F_{sand}, which indicates the feasibility of using fractal dimension parameters to estimate wilting point (Figure 7, Supplementary 4). The wilting point had a stronger correlation with clay content than with biomass, whereas the correlation between the wilting point and biomass was significant at the 0.01 level (2-tailed) (Supplementary 4). This correlation may exist because there is little variation in clay content over small scales at which the influences of the vegetation appear. This result suggests that clay content rather than vegetation condition is the main factor correlated with the wilting point, and the fitting efficiency of the clay content to the wilting point is very good in practice (Wang and Shao, 2000).

Clay content is more strongly correlated with fractal dimension than is silt content or sand content. Both cultivation and natural movement by wind, water or gravity impact the soil particle-size distribution (Dong and Zheng, 2009; Gui et al., 2010; Wang et al., 2007; Xia et al., 2015; Zhao et al., 2015). The singular dimension has a stronger correlation with position at the transect scale, while the multiple dimension has a stronger correlation with the gradient (Supplementary 4). Biomass shows a significant correlation with soil particle size uniformity, F in the silt domain and F in the clay domain, which also indicates that fine particles have a greater impact on plants than coarse particles (Supplementary 4). In addition, the impact of biomass on wilting point is greater than its impact on soil water content, and biomass has a positive correlation with soil water content in the 0-1-m soil layers and a negative correlation in the 2-5-m soil layers (Figure 7), indicating that greater plant biomass could reduce soil water loss in shallow layers through reduced evaporation while increasing soil water consumption in deep soil layers.

Fractal dimensions have been used to estimate the soil-water characteristic curve, which simplifies the fitting process (Tyler and Wheatcraft, 1989, 1990, 1992; Zheng et al., 2012). In this study, although the overall simulation results are good, some of the modeled soil water content conditions in the lower layers are slightly higher than the measured values (Figure 4). While it is feasible to study the relationships between soil properties and soil hydraulic properties using this approach, the model must be calibrated under different soil water contents and soil particle-size distributions.

5. Conclusion

Research on ecological restoration is important on the Loess Plateau of China because of the severe soil and water conservation challenges in this region. In the context of global climate change, the frequency of

extreme weather years (drought or flood) may increase. The soil water content and soil particle-size distribution on the sampled slopes vary with position along the slope and with soil depth. From the upper part of the slope to the lower part, soil water content increases inconsistently, and the singular fractal dimension and D_0 positively correlate with the soil water content on the shrubland slopes, while these changes are not consistent on the grassland slope. From the shallow soil layers to the deep soil layers, the change in singular fractal dimension is positively correlated with soil water content, while D_0 is negatively correlated with soil water content with increasing depth. The biomass exhibits a positive correlation with soil water content in the 0-100-cm soil layers, but the correlation becomes negative in the 200-500-cm soil layers. The change in the wilting point is related to both biomass and the proportion of fine soil particles at the transect scale.

Estimation of the soil-water characteristic curve using easily obtainable soil parameters is feasible. During a drought year, the soil water that can be used by *Caragana* is below 2 m, while the soil water that can be used by grass is below 1.2 m. Although CK has greatly contributed to local soil and water conservation in the last century, extensive and long-term planting of this shrub species is not suitable for sustainable vegetation restoration on the Loess Plateau as the climate may change due to both future warming and drying conditions. For south-facing slopes, which have lower soil water contents than the north-facing slopes, leaving the upper slope to naturally revegetate with grasses to maintain soil water while planting CK lower on the slope to retain fine soil particles may be a better vegetation restoration approach. This special region of drylands occupies a large area; therefore, these suggestions to balance water consumption and soil erosion might be used for vegetation restoration in other semiarid areas with thick soil layers and deep ground water.

Acknowledgements

This work was supported by the National Natural Science Foundation of China (Nos. 41390462, 41771197) and the State Key Laboratory of Earth Surface Processes and Resource Ecology(No.2017-FX-01(2)).

References

Andraud, C., A. Beghdadi, E. Haslund, R. Hilfer, J. Lafait, and B. Virgin. 1997. Local entropy characterization of correlated random microstructures. Physica A 235:307–318. doi:10.1016/s0378-4371(96)00354-8

Andraud, C., A. Beghdadi, and J. Lafait. 1994. Entropic analysis of random morphologies. Physica A 207:208–212. doi:10.1016/0378-4371(94)90374-3

Arya, L.M., and J.F. Paris. 1981. A physicoempirical model to predict the soil moisture characteristic from particle-size distribution and bulk density data. Soil Sci. Soc. Am. J. 45:1023–1030. doi:10.2136/sssaj1981.03615995004500060004x

Bai, Y., and Y. Wang. 2012. Monofractal and multifractal analysis on soil particle distribution in hilly and gully areas of the Loess Plateau. Trans. Chin. Soc. Agric. Mach. 43:42–48. doi:10.6041/j.issn.1000-1298.2012.05.008

Brooks, R.H., and A.T. Corey. 1964. Hydraulic properties of porous media: Hydrology papers. Colorado State University, Fort Collins.

Campbell, G.S. 1974. A simple method for determining unsaturated conductivity from moisture retention data. Soil Sci. Soc. Am. J. 117:311–314. doi:10.1097/00010694-197406000-00001

Carsel, R.F., and R.S. Parrish. 1988. Developing joint probability distributions of soil water retention characteristics. Water Resour. Res. 24:755–769. doi:10.1029/wr024i005p00755

Chen, H., M. Shao, and Y. Li. 2008. The characteristics of soil water cycle and water balance on steep grassland under natural and simulated rainfall conditions in the Loess Plateau of China. J. Hydrol. 360:242–251. doi:10.1016/j.jhydrol.2008.07.037

Cortina, J. and F. T. Maestre. 2005. Plant effects on soils in drylands: implications for community dynamics and ecosystem restoration. Tree species effects on soils: implications for global change. Dordrecht, Springer: 85-118.

Daly, K.R., S.J. Mooney, M.J. Bennett, N.M.J. Crout, T. Roose, and S.R. Tracy. 2015. Assessing the influence of the rhizosphere on soil hydraulic properties using X-ray computed tomography and numerical modelling. J. Exp. Bot. 66:2305–2314. doi:10.1093/jxb/eru509

Dong, L., and F. Zheng. 2009. Fractal charateristics of soil particles in the hilly-gully regions of the Loess Plateau, north of Shaanxi, China. Science of Soil and Water Conservation 7:35–41.

Dong, L., and F. Zheng. 2010. Fractal characteristics of soil particle size distributions in Gully-hilly regions of the Loess Plateau, north of Shaanxi, China. Soils 42:302–308.

Fang, X., W. Zhao, L. Wang, Q. Feng, J. Ding, Y. Liu, et al. 2016. Variations of deep soil moisture under different vegetation types and influencing factors in a watershed of the Loess Plateau, China. Hydrol. Earth Syst. Sci. 20:3309–3323. doi:10.5194/hess-20-3309-2016

Fu, B. 1989. Soil erosion and its control in the loess plateau of China. Soil Use and Management 5:76-82.

Fu, B., L. Chen, Y. Qiu, J. Wang, and Q. Meng. 2002. Landuse structure and ecologyical process in the Loess gullly region. The Commercial Press, Beijing.

Gao, X., P. Wu, B. Zhang, J. Huang, and X. Zhao. 2015. Spatial variability of avaliable soil moisture and its seasonality in a small watershed in the hilly region of the Loess Plateau. Pedologica 52:57–67. doi:10.11766/trxb201404040151

Gao, X., P. Wu, X. Zhao, Y. Shi, J. Wang, and B. Zhang. 2011. Soil moisture variability along transects over a well-developed gully in the Loess Plateau, China. Catena 87:357–367. doi:10.1016/j.catena.2011.07.004

Gouyet, J.-F. 1996. Physics and fractal structures. Masson Springer, Paris New York.

Grout, H., A.M. Tarquis, and M.R. Wiesner. 1998. Multifractal analysis of particle size distributions in soil. Environ. Sci. Technol. 32:1176–1182. doi:10.1021/es9704343

Gu, Z. and H. Luo. 2016. Effects of three-dimensional structure of vegetation on particle size distribution and nutrient content of water-eroded red soil. Agricultural Science & Technology 17(2): 453-459, 466.

Gui, D., J. Lei, F. Zeng, G. Mu, J. Zhu, H. Wang, et al. 2010a. Characterizing variations in soil particle size distribution in oasis farmlands—A case study of the Cele Oasis. Mathematical and Computer Modelling 51:1306–1311. doi:10.1016/j.mcm.2009.10.035

Hopmans, J.W., and J. Simunek. 1999. Review of inverse estimation of soil hydraulic properties. In: T.V. Genuchten,

F.J. Leij and L. Wu, editors, Int. workshop Characterization and Management of the Hydraulic Properties of Unsaturated Porous Media. University of California, Riverside, CA, USA. p. 643–659.

Huang, J., P. Wu, and X. Zhao. 2013. Effects of rainfall intensity, underlying surface and slope gradient on soil infiltration under simulated rainfall experiments. Catena 104:93–102. doi:10.1016/j.catena.2012.10.013

Jiao, F., Z. Wen, J. Jiao, and X. He. 2006. Reciprocal effects among vegetation, soil moisture and nutrients of cropland to forest and grassland in the Loess Hilly Region. Acta Prataculturae Sinica 15:79–84.

Jiménez, J.J., R. Lal, R.O. Russo, and H.A. Leblanc. 2008. The soil organic carbon in particle-size separates under different regrowth forest stands of north eastern Costa Rica. Ecological Engineering 34:300–310. doi:10.1016/j.ecoleng.2008.07.001

Jin, Z., Y.S. Dong, Y.C. Qi, W.G. Liu, and Z.S. An. 2013. Characterizing variations in soil particle-size distribution along a grass-desert shrub transition in the Ordos plateau of inner Mongolia, China. Land Degradation & Development 24:141–146. doi:10.1002/ldr.1112

Khanzode, R.M., S.K. Vanapalli, and D.G. Fredlund. 2002. Measurement of soil-water characteristic curves for fine-grained soils using a small-scale centrifuge. Can. Geotech. J. 39:1209–1217. doi:10.1139/t02-060

Keith, L., Heppner, C. S., Mirus, B. B., Ebel B. A., Ran, Q., Carr, A. E., BeVille, S. H., and VanderKwaak J. E. 2006. Physics-based hydrologic-response simulation: Foundation for hydroecology and hydrogeomorphology. Hydrol. Pro. 20: 1231-1237.

Kong, Y., and E. Song. 2015. A method for estimating soil-water characteristic curve from grain-size distribution. Rock Soil Mech. 36:2487–2493. doi:10.16285/j.rsm.2015.09.007

Lai, J., and Q. Wang. 2003. Comparison of soil water retenrion curve model. J. Soil Water Conserv. 17:137–140.

Li, D., G. Gao, M.A. Shao, and B. Fu. 2016. Predicting available water of soil from particle-size distribution and bulk density in an oasis–desert transect in northwestern China. J. Hydrol. 538:539–550. doi:10.1016/j.jhydrol.2016.04.046

Li, W., M. Yan, Z. Qingfeng and J. Zhikaun. 2012. Effects of Vegetation Restoration on Soil Physical Properties in the Wind-Water Erosion Region of the Northern Loess Plateau of China. CLEAN - Soil, Air, Water 40(1): 7-15.

Lin, H. 2010. Earth's critical zone and hydropedology: Concepts, characteristics, and advances. Hydrol. Earth Syst. Sci. 14:25–45. doi:10.5194/hess-14-25-2010

Lin, H. 2011. Hydropedology: Towards new insights into interactive pedologic and hydrologic processes across scales. J. Hydrol. 406:141–145. doi:10.1016/j.jhydrol.2011.05.054

Liu, J., and S. Xu. 2003. Figuring soil water characteristic curve based on particle size distribution data: Application of fractal models. Acta Pedologica Sinica 40:46–52.

Liu, S., X. Guo, G. Lian, and J. Wamh. 2007. Multi-scale ecological security evaluation of typical fragile areas in Loess Plateau. Chin. J. Appl. Ecol. 18:1554–1559.

Liu, Y., P. Wang, Y. Ding, H. Lu, L. Li, K. Cheng, et al. 2016a. Microbial activity promoted with organic carbon accumulation in macroaggregates of paddy soils under long-term rice cultivation. Biogeosciences 13:6565–6586. doi:10.5194/bg-13-6565-2016

Liu, Y., W. Zhao, L. Wang, X. Zhang, S. Daryanto, and X. Fang. 2016b. Spatial variations of soil moisture under Caragana korshinskii Kom. from different precipitation zones: Field based analysis in the Loess Plateau, China. Forests 7:31. doi:10.3390/f7020031

Lü, Y., B. Fu, X. Feng, Y. Zeng, Y. Liu, R. Chang, et al. 2012. A policy-driven large scale ecological restoration: Quantifying ecosystem services changes in the Loess Plateau of China. PLoS One 7:e31782. doi:10.1371/journal.pone.0031782

Lü, Y., Z. Ma, Z. Zhao, F. Sun, and B. Fu. 2014a. Effects of land use change on soil carbon storage and water consumption in an Oasis-desert ecotone. Environ. Manage. 53:1066–1076. doi:10.1007/s00267-014-0262-6

Lü, Y., F. Sun, J. Wang, Y. Zeng, M. Holmberg, K. Böttcher, et al. 2014b. Managing landscape heterogeneity in different socio-ecological contexts: Contrasting cases from central Loess plateau of China and southern Finland. Landscape Ecology 30:463–475. doi:10.1007/s10980-014-0129-5

Lü, Y., L. Zhang, X. Feng, Y. Zeng, B. Fu, X. Yao, et al. 2015. Recent ecological transitions in China: Greening, browning, and influential factors. Sci. Rep. 5:8732. doi:10.1038/srep08732

Marinho, M.A., M.W.M. Pereira, E.V. Vázquez, M. Lado, and A.P. González. 2017. Depth distribution of soil organic carbon in an Oxisol under different land uses: Stratification indices and multifractal analysis. Geoderma 287:126–134. doi:10.1016/j.geoderma.2016.09.021

Marques, J.D.D.O., F.J. Luizão, W.G. Teixeira, M. Sarrazin, S.J.F. Ferreira, T.P. Beldini, et al. 2015. Distribution of organic carbon in different soil fractions in ecosystems of central Amazonia. Rev. Bras. Cienc. Solo 39:232–242. doi:10.1590/01000683rbcs20150142

Meskini-Vishkaee, F., M.H. Mohammadi, and M. Vanclooster. 2014. Predicting the soil moisture retention curve, from soil particle size distribution and bulk density data using a packing density scaling factor. Hydrol. Earth Syst. Sci. 18:4053–4063. doi:10.5194/hess-18-4053-2014

Mirus, B.B., K.S. Perkins, J.R. Nimmo, and K. Singha. 2009. Hydrologic characterization of desert soils with varying degrees of pedogenesis: 2. Inverse modeling for effective properties. Vadose Zone J. 8:496–509. doi:10.2136/vzj2008.0051

Montenegro, S., and R. Ragab. 2012. Impact of possible climate and land use changes in the semi arid regions: A case study from North Eastern Brazil. J. Hydrol. 434–435:55–68. doi:10.1016/j.jhydrol.2012.02.036

Montero, E.S. 2005. Rényi dimensions analysis of soil particle-size distributions. Ecol. Modell. 182:305–315. doi:10.1016/j.ecolmodel.2004.04.007

Nguyen, H.Y.T., D.M. Cao, and K. Schmitt. 2012. Soil particle-size composition and coastal erosion and accretion study in Soc Trang mangrove forests. Journal of Coastal Conservation 17:93–104. doi:10.1007/s11852-012-0221-4

Nimmo, J.R., and K.A. Mello. 1991. Centrifugal techniques for measuring saturated hydraulic conductivity. Water Resour. Res. 27:1263–1269. doi:10.1029/91WR00367.

Nimmo, J.R., J. Rubin, and D.P. Hammermeister. 1987. Unsaturated flow in a centrifugal field: Measurement of hydraulic conductivity and testing of Darcy's Law. Water Resour. Res. 23:124–134. doi:10.1029/wr023i001p00124

Ning, T., Z. Guo, M. Guo, and B. Han. 2013. Soil water resources use limit in the loess plateau of China. Agric. Sci. 4:100–105. doi:10.4236/as.2013.45b019

Peitgen, H.O., H. Jürgens, and D. Saupe. 1992. Chaos and fractals: New frontiers of science. Springer-Verlag, New York, NY.

Peng, G., N. Xiang, S.-Q. Lv, and G.-C. Zhang. 2014. Fractal characterization of soil particle-size distribution under different land-use patterns in the Yellow river delta wetland in China. J. Soils Sediments 14:1116–1122. doi:10.1007/s11368-014-0876-6

Peng, H., R. Horton, T. Lei, Z. Dai, and X. Wang. 2015. A modified method for estimating fine and coarse fractal dimensions of soil particle size distributions based on laser diffraction analysis. J. Soils Sediments 15:937–948. doi:10.1007/s11368-014-1044-8

Posadas, A.N.D., D. Giménez, M. Bittelli, C.M.P. Vaz, and M. Flury. 2001. Multifractal characterization of soil particle-size distributions. Soil Sci. Soc. Am. J. 65:1361. doi:10.2136/sssaj2001.6551361x

Qin, D., T. Stocker, 259 Authors and Tsu (in Bern & Beijing). 2014. Highlights of the IPCC Working Group I Fifth Assessment Report. Progress Inquisitiones de Mutatione Climates, 10:1–6.

Qin, D.H., Y.H. Din, S.W. Wang, S.M. Wang, G.R. Dong, E.D. Lin, et al. 2002. Ecological and environmental change in west China and its response strategy. Advances in Earth Science 17:314–319.

Qiu, Y., B. Fu, J. Wang, and L. Chen. 2001. Soil moisture variation in relation to topography and land use in a hillslope catchment of the Loess Plateau, China. J. Hydrol. 240:243–263. doi:10.1016/s0022-1694(00)00362-0

Reatto, A., E.M. da Silva, A. Bruand, E.S. Martins, and J.E.F.W. Lima. 2008. Validity of the centrifuge method for determining the water retention properties of tropical soils. Soil Sci. Soc. Am. J. 72:1547. doi:10.2136/sssaj2007.0355n

Ru, H., J. Zhang, Y. Li, Z. Yang, and H. Feng. 2015. Fractal features of soil particle size distributions and its effect on soil erosion of Loess Plateau. Trans. Chin. Soc. Agric. Mach. 46:176–182.

Schaap, M.G., F.J. Leij, and M.T. van Genuchten. 2001. ROSETTA: A computer program for estimating soil hydraulic parameters with hierarchical pedotransfer functions. J. Hydrol. 251:163–176. doi:10.1016/s0022-1694(01)00466-8

Shannon, C.E. 2001. A mathematical theory of communication. ACM SIGMOBILE Mobile Computing and Communications Review 5:3–55. doi:10.1145/584091.584093

Shao, M., Y. Wang, and X. Jia. 2015. Ecological Construction and Soil Desiccation on the Loess Plateau of China. Bulletin of Chinese Academy of Sciences. 30(Z1): 178-185 (in Chinese with English abstract)

Shao, M., Q. Wang, and M. Huang. 2006. Soil physics. Higher Education Press, Beijing.

Shi, H., and M. Shao. 2000. Soil and water loss from the Loess Plateau in China. Journal of Arid Environments 45:9-20.

Song, X.Y., and H.Y. Li. 2011. Fractal characteristics of soil particle-size distributions under different landform and land-use types. Adv. Mater. Res. 201-203:2679–2684. doi:10.4028/www.scientific.net/amr.201-203.2679

Song, Z., C. Zhang, G. Liu, D. Qu, and S. Xue. 2015. Fractal feature of particle-size distribution in the rhizospheres

and bulk soils during natural recovery on the Loess plateau, China. PLoS One 10:e0138057. doi:10.1371/journal.pone.0138057

Stocker, T.F., D. Qin, G.-K. Plattner, M. Tignor, S.K. Allen, J. Boschung, et al. 2013. IPCC, 2013: Climate change 2013: The physical science basis. Contribution of working group I to the fifth assessment report of the intergovernmental panel on climate change. Cambridge University Press, Cambridge, United Kingdom and New York, NY, USA.

Sun, C., G. Liu and S. Xue. 2016a. "Land-Use Conversion Changes the Multifractal Features of Particle-Size Distribution on the Loess Plateau of China." Int J Environ Res Public Health 13(8):785.

Sun, C., G. Liu, and S. Xue. 2016b. Natural succession of grassland on the Loess plateau of China affects multifractal characteristics of soil particle-size distribution and soil nutrients. Ecol. Res. 31:891–902. doi:10.1007/s11284-016-1399-y

Tyler, S.W., and S.W. Wheatcraft. 1989. Application of fractal mathematics to soil water retention estimation. Soil Sci. Soc. Am. J. 53:987–996. doi:10.2136/sssaj1989.03615995005300040001x

Tyler, S.W., and S.W. Wheatcraft. 1990. Fractal processes in soil water retention. Water Resour. Res. 26:1047–1054. doi:10.1029/wr026i005p01047

Tyler, S.W., and S.W. Wheatcraft. 1992. Fractal scaling of soil particle-size distributions: Analysis and limitations. Soil Sci. Soc. Am. J. 56:362–369. doi:10.2136/sssaj1992.03615995005600020005x

van Genuchten, M.T. 1980. A closed-form equation for predicting the hydraulic conductivity of unsaturated soils. Soil Sci. Soc. Am. J. 44:892–898. doi:10.2136/sssaj1980.03615995004400050002x

Venkatesh, B., N. Lakshman, B.K. Purandara, and V.B. Reddy. 2011. Analysis of observed soil moisture patterns under different land covers in Western Ghats, India. J. Hydrol. 397:281–294. doi:10.1016/j.jhydrol.2010.12.006

Vereecken, H., M. Weynants, M. Javaux, Y. Pachepsky, M.G. Schaap, and M.T.V. Genuchten. 2010. Using pedotransfer functions to estimate the van Genuchten–Mualem soil hydraulic properties: A review. Vadose Zone J. 9:795. doi:10.2136/vzj2010.0045

Vivoni, E.R. 2012. Diagnosing seasonal vegetation impacts on evapotranspiration and its partitioning at the catchment scale during SMEX04–NAME. Journal of Hydrometeorology 13:1631–1638. doi:10.1175/jhm-d-11-0131.1

Voss, R.F. 1988. Fractals in nature: From characterization to simulation. In: H.-O. Peitgen and D. Saupe, editors, The science of fractal images. Springer New York, New York, NY. p. 21–70.

Vrugt, J.A., P.H. Stauffer, T. Wöhling, B.A. Robinson, and V.V. Vesselinov. 2008. Inverse modeling of subsurface flow and transport properties: A review with new developments. Vadose Zone J. 7:843. doi:10.2136/vzj2007.0078

Wang, B., G.B. Liu, S. Xue, and B. Zhu. 2010. Changes in soil physico-chemical and microbiological properties during natural succession on abandoned farmland in the Loess Plateau. Environ. Earth Sci. 62:915–925. doi:10.1007/s12665-010-0577-4

Wang, B., F. Wen, J. Wu, X. Wang, and Y. Hu. 2014. Vertical profiles of soil water content as influenced by

environmental factors in a small catchment on the Hilly-Gully Loess plateau. PLoS One 9:e109546. doi:10.1371/journal.pone.0109546

Wang, D., B. Fu, L. Chen, W. Zhao, and Y. Wang. 2007. Fractal analysis on soil particle size distributions under different land-use types: A case study in the Loess hilly areas of the Loess Plateau, China. Acta Ecologica Sinica 27:3081–3089.

Wang, L., P. D'Odorico, J. Evans, D. Eldridge, M. McCabe, K. Caylor, and E. King. 2012. Dryland ecohydrology and climate change: critical issues and technical advances. Hydrology and Earth System Sciences **16**:2585-2603.

Wang, S., G.C. van Kooten, and B. Wilson. 2004. Mosaic of reform: Forest policy in post-1978 China. Forest Policy and Economics 6:71–83. doi:10.1016/s1389-9341(02)00078-3

Wang, W., and M.A. Shao. 2000. Research of soil moisture in the Loess Plateau. Science Press, Beijing.

Wang, X., K. Jia, J. Liu, and L. Li. 2009a. Application of van Genuchten model to analysis of soil moisture charateristic curve. Agricultural Research in the Arid Areas 27:179–183.

Wang, Y., M.A. Shao, and Z. Liu. 2013. Vertical distribution and influencing factors of soil water content within 21-m profile on the Chinese Loess Plateau. Geoderma 193-194:300–310. doi:10.1016/j.geoderma.2012.10.011

Wang, Y., M.A. Shao, Y. Zhu, and Z. Liu. 2011. Impacts of land use and plant characteristics on dried soil layers in different climatic regions on the Loess Plateau of China. Agric. For. Meteorol. 151:437–448. doi:10.1016/j.agrformet.2010.11.016

Wang, Z., B. Liu, and Y. Zhang. 2009b. Soil moisture of different vegetation types on the Loess Plateau. Journal of Geographical Sciences 19:707–718. doi:10.1007/s11442-009-0707-7

Xia, D., Y. Deng, S. Wang, S. Ding, and C. Cai. 2015. Fractal features of soil particle-size distribution of different weathering profiles of the collapsing gullies in the hilly granitic region, south China. Natural Hazards 79:455–478. doi:10.1007/s11069-015-1852-1

Yan, W., L. Deng, Y. Zhong, and Z. Shangguan. 2015. The characters of dry soil layer on the Loess Plateau in China and their influencing factors. PLoS One 10:e0134902. doi:10.1371/journal.pone.0134902

Yang, J., D. Li, G. Zhang, Y. Zhao, W. Zhao, and X. Tang. 2008. Comparison of mass and volume fractal dimensions of soil particle size distributions. Acta Pedol. Sin. 45:413–419.

Yang, L., L. Chen, W. Wei, Y. Yu, H. Zhang. 2014a. Comparison of deep soil moisture in two re-vegetation watersheds in semi-arid regions. Journal of Hydrology 513:314-321. doi: 10.1016/j.jhydrol.2014.03.049

Yang, L., W. Wei, L. Chen, W. Chen, and J. Wang. 2014b. Response of temporal variation of soil moisture to vegetation restoration in semi-arid Loess Plateau, China. Catena 115:123–133. doi:10.1016/j.catena.2013.12.005

Yao, X., B. Fu, Y. Lü, R. Chang, S. Wang, Y. Wang, et al. 2012. The multi-scale spatial variance of soil moisture in the semi-arid Loess Plateau of China. J. Soils Sediments 12:694–703. doi:10.1007/s11368-012-0481-5

Yu, J., X. Lv, M. Bin, H. Wu, S. Du, M. Zhou, et al. 2015a. Fractal features of soil particle size distribution in newly formed wetlands in the Yellow River Delta. Sci. Rep. 5:10540. doi:10.1038/srep10540

Yu, Y., W. Wei, L.D. Chen, F.Y. Jia, L. Yang, H.D. Zhang, et al. 2015b. Responses of vertical soil moisture to rainfall

pulses and land uses in a typical Loess hilly area, China. Solid Earth 6:595–608. doi:10.5194/se-6-595-2015

Zaffar, M., and S.-G. Lu. 2015. Pore size distribution of clayey soils and its correlation with soil organic matter. Pedosphere 25:240–249. doi:10.1016/s1002-0160(15)60009-1

Zhang, J., G. Li, Z. Nan, and H. Xiao. 2012b. Research on soil particle size distribution and its relationship with soil prganic carbon under the effects of tillage in the Heihe oasis. Geographical Research 31(4):608-618.

Zhang, J., G. Li, and Z. Nan. 2012a. Soil particle size distribution and its relationship with soil organic carbons under different land uses in the middle of Heihe river. Acta Ecologica Sinica 32:3745–3753. doi:10.5846/stxb201110091473

Zhang, Q., X. Jia, C. Zhao and M. Shao. 2018. Revegetation with artificial plants improves topsoil hydrological properties but intensifies deep-soil drying in northern Loess Plateau, China. Journal of Arid Land 10(3): 335-346.

Zhang, X., W. Zhao, Y. Liu, X. Fang, and Q. Feng. 2016a. The relationships between grasslands and soil moisture on the Loess Plateau of China: A review. Catena 145:56–67. doi:10.1016/j.catena.2016.05.022

Zhang, X., W. Zhao, Y. Liu, X. Fang, Q. Feng, and Z. Chen. 2016b. Spatial variations and impact factors of soil water content in typical natural and artificial grasslands: A case study in the Loess Plateau of China. J. Soils Sediments 17:157–171. doi:10.1007/s11368-016-1505-3

Zhao, M., and S.W. Running. 2010. Drought-induced reduction in global terrestrial net primary production from 2000 through 2009. Science 329:940–943. doi:10.1126/science.1192666

Zhao, M., W. Zhao, and Y. Liu. 2015. Comparative analysis of soil particle size distribution and its influence factors in different scales: A case study in the Loess Plateau of China. Acta Ecologica Sinica 35. doi:10.5846/stxb201311272828

Zhao, M., W. Zhao, and L. Zhong. 2014. Scale effect analysis of the influence of land use and environmental factors on surface soil organic carbon：A case study in the hilly and gully area of Northern Shaanxi province. Acta Ecologica Sinica 34:1105–1113. doi:10.5846/stxb201306101597

Zhao, P., M.-A. Shao, and R. Horton. 2011. Performance of soil particle-size distribution models for describing deposited soils adjacent to constructed dams in the China Loess Plateau. Acta Geophys. 59. doi:10.2478/s11600-010-0037-2

Zheng, Z., W. Li, T. Li, H. Yu, and L. Zeng. 2012. Soil water retention curve based on fractal theory in greenhouse soil. Trans. Chin. Soc. Agric. Mach. 43:49–54.

Tables

Table 1 Soil property index values at different slope positions.

Index (unit)	Position	Mean value	95% confidence interval of mean		Min	Max
			Lower limit	Upper limit		
d(0.1) (μm)	Lower	3.69 ± 0.75a	3.53	3.86	2.31	6.03
	Middle	4.22 ± 0.79b	4.05	4.39	2.79	5.87
	Upper	4.59 ± 0.94c	4.39	4.80	3.11	7.01
d(0.5) (μm)	Lower	31.62 ± 4.54a	30.61	32.62	23.58	49.07
	Middle	33.90 ± 4.54b	32.90	34.90	25.38	44.25
	Upper	36.24 ± 5.52c	35.02	37.46	26.20	53.74
d(0.9) (μm)	Lower	77.69 ± 9.52a	75.58	79.79	31.55	104.72
	Middle	81.97 ± 8.57b	80.07	83.86	67.94	107.74
	Upper	85.86 ± 13.61c	82.85	88.87	67.45	173.82
R	Lower	0.21 ± 0.02a	0.21	0.22	0.12	0.26
	Middle	0.22 ± 0.02b	0.21	0.22	0.17	0.27
	Upper	0.22 ± 0.02b	0.22	0.23	0.17	0.28
Sand (%)	Lower	28.49 ± 5.45a	27.28	29.69	19.51	49.15
	Middle	30.99 ± 5.47b	29.78	32.20	21.28	43.65
	Upper	33.64 ± 6.59c	32.19	35.10	21.74	52.52
Silt (%)	Lower	68.49 ± 5.18a	67.34	69.63	49.01	76.65
	Middle	66.26 ± 5.25b	65.09	67.42	53.78	75.68
	Upper	63.78 ± 6.37c	62.37	65.19	45.81	75.31
Clay (%)	Lower	3.03 ± 0.60a	2.90	3.16	1.84	4.79
	Middle	2.75 ± 0.46b	2.65	2.85	1.94	4.14
	Upper	2.58 ± 0.43c	2.49	2.68	1.68	3.56
SWC (g/g)	Lower	0.07 ± 0.04a	0.06	0.08	0.02	0.19
	Middle	0.06 ± 0.03b	0.05	0.06	0.02	0.13
	Upper	0.05 ± 0.03b	0.04	0.05	0.02	0.13

Note: The same lowercase letters in the same columns indicate that the differences are not significant at the 0.05 level (one-way ANOVA and LSDM test; SWC represents soil water content). d(0.1) means the mass of the particles with sizes smaller than this value constitute 10% of the total mass; d(0.5) indicates the mass median diameter (MMD), which is also called the log-normal distribution mass median diameter; d(0.9) means the mass of the particles with sizes smaller than this value constitute 90% of the total mass; R indicates *D[3,2]/D[3,4]* (Sauter mean diameter / volume-based mean diameter) and the value following "±" is the standard error of the mean.

Table 2 Fitting parameters, wilting points, soil water contents and bulk densities of the soil samples.

Position	Depth (cm)	Fitting parameters				Wilting point (g/g)	SWC (g/g)	Bulk density (g/cm^3)
		θ_s	θ_r	α	n			
Slope 2								
Upper slope	0-40	0.06	0.38	20.74	1.95	0.06	0.02	1.353
	40-80	0.06	0.38	22.16	1.88	0.06	0.03	1.34
	80-120	0.05	0.37	21.11	1.88	0.05	0.03	1.38
	120-200	0.05	0.37	18.99	1.83	0.06	0.04	1.33
Middle slope	0-40	0.06	0.31	14.39	1.77	0.06	0.04	1.28
	40-80	0.07	0.39	18.38	1.80	0.07	0.05	1.29
	80-120	0.07	0.39	19.01	1.76	0.07	0.05	1.30
	120-200	0.08	0.38	19.33	1.62	0.09	0.06	1.33
Lower slope	0-40	0.07	0.35	15.50	1.61	0.08	0.04	1.32
	40-80	0.08	0.38	17.27	1.75	0.08	0.06	1.33
	80-120	0.08	0.39	20.09	1.68	0.09	0.07	1.35
	120-200	0.08	0.36	17.58	1.62	0.09	0.08	1.37
Slope 3								
Upper slope	0-40	0.06	0.33	16.79	1.85	0.06	0.03	1.08
	40-80	0.05	0.36	21.54	1.91	0.06	0.04	1.26
	80-120	0.05	0.35	18.15	1.88	0.06	0.05	1.37
	120-200	0.06	0.37	15.46	1.90	0.06	0.09	1.33
Middle slope	0-40	0.06	0.34	17.30	1.89	0.06	0.03	1.34
	40-80	0.05	0.35	19.87	1.91	0.05	0.03	1.42
	80-120	0.05	0.35	19.63	1.77	0.05	0.04	1.36
	120-200	0.06	0.36	18.39	1.77	0.06	0.08	1.33
Lower slope	0-40	0.05	0.33	19.53	1.76	0.06	0.03	1.23
	40-80	0.05	0.36	20.89	1.83	0.06	0.04	1.36
	80-120	0.06	0.37	20.67	1.87	0.06	0.05	1.45
	120-200	0.06	0.40	22.09	1.71	0.06	0.08	1.35

Note: θ_s, θ_r, α, n are fitting parameters in the van Genuchten model (Equation 1); SWC represents soil water content.

Highlights

- Fractal dimension analysis is a useful tool for understanding hydropedology.
- Shrub and grass used soil water below 2 m and 1.2 m respectively in a drought year.
- Shrub reduces erosion of fine particles but consumes water stored in deep layers.

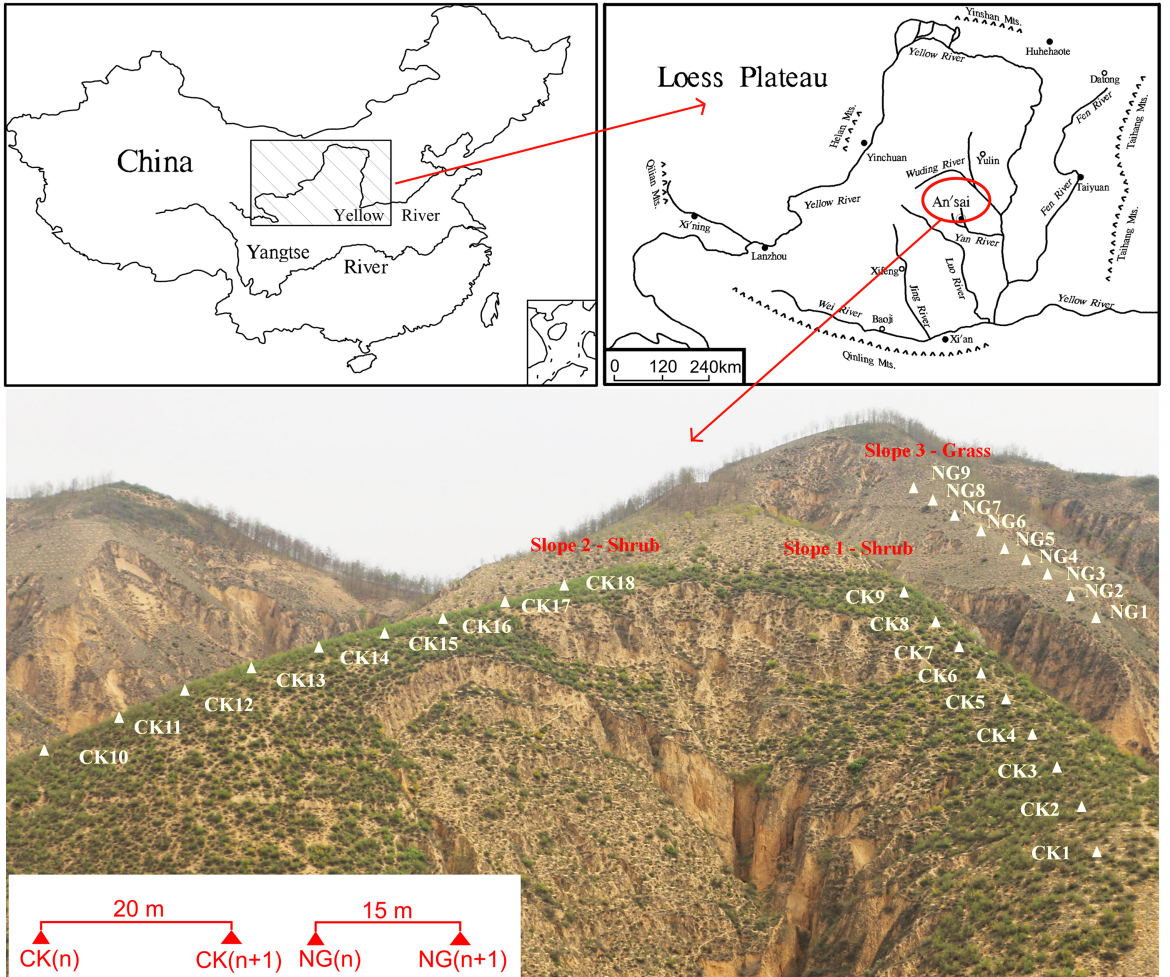
China
Yellow River
Yangtse River
Loess Plateau
Yinshan Mts.
Yellow River
Huhehaote
Datong
Helan Mts.
Yinchuan
Wuding River
Yulin
Fen River
Taihang Mts.
Qilian Mts.
Xining
Yellow River
An'sai
Taiyuan
Fen River
Lanzhou
Yan River
Xifeng
Luo River
Jing River
Taihang Mt.
Wei River
Baoji
Yellow River
Xi'an
Qinling Mts.
0 120 240km
Slope 3 - Grass
NG9
NG8
NG7
NG6
NG5
NG4
NG3
NG2
NG1
Slope 2 - Shrub
Slope 1 - Shrub
CK18
CK17
CK16
CK15
CK14
CK13
CK12
CK11
CK10
CK9
CK8
CK7
CK6
CK5
CK4
CK3
CK2
CK1
20 m
15 m
CK(n)
CK(n+1)
NG(n)
NG(n+1)

Figure 1

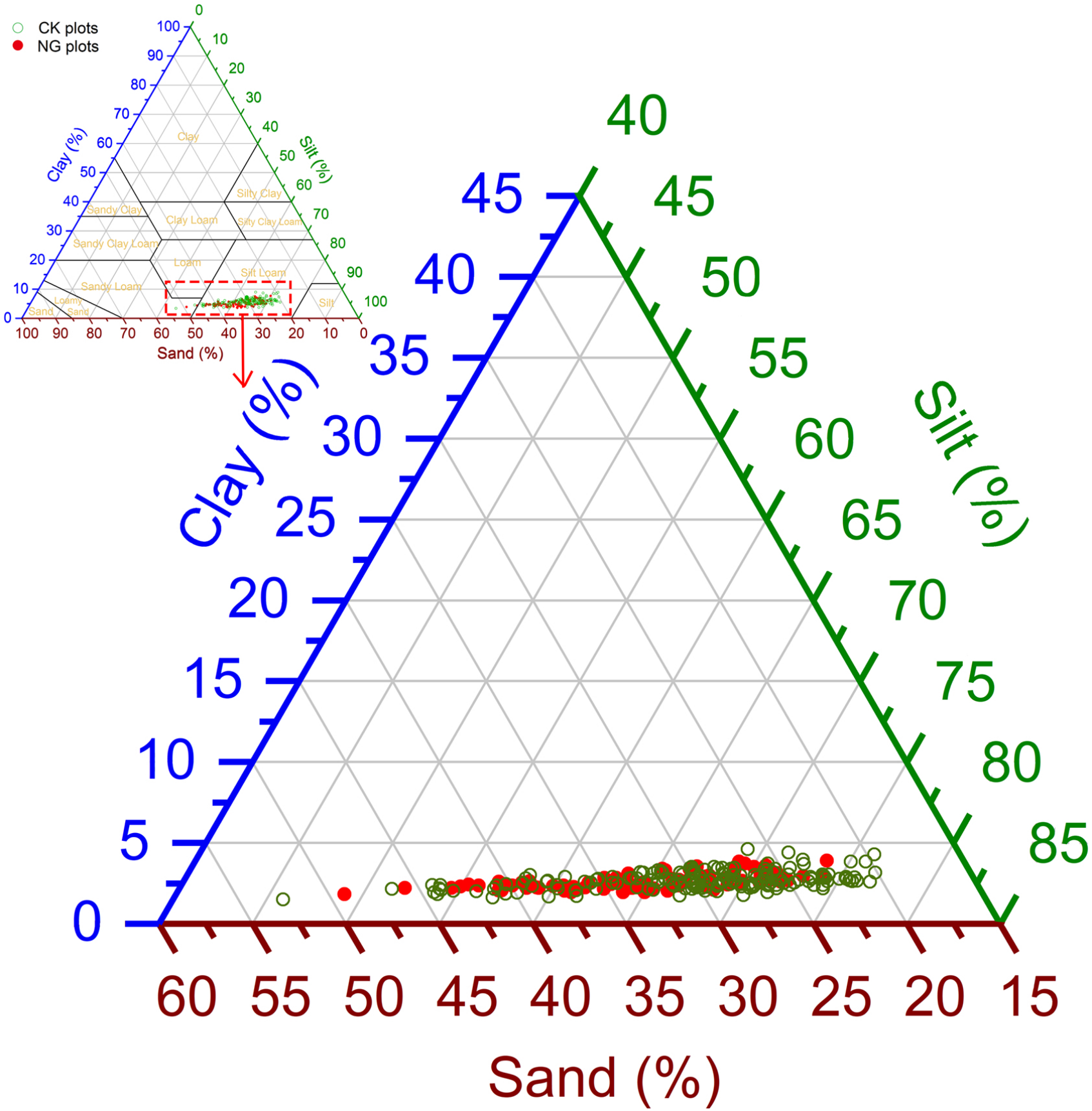
CK plots
NG plots
Clay (%)
Silt (%)
Sand (%)
Clay
Silty Clay
Sandy Clay
Clay Loam
Silty Clay Loam
Sandy Clay Loam
Loam
Silt Loam
Sandy Loam
Loamy Sand
Sand
Silt

Figure 2

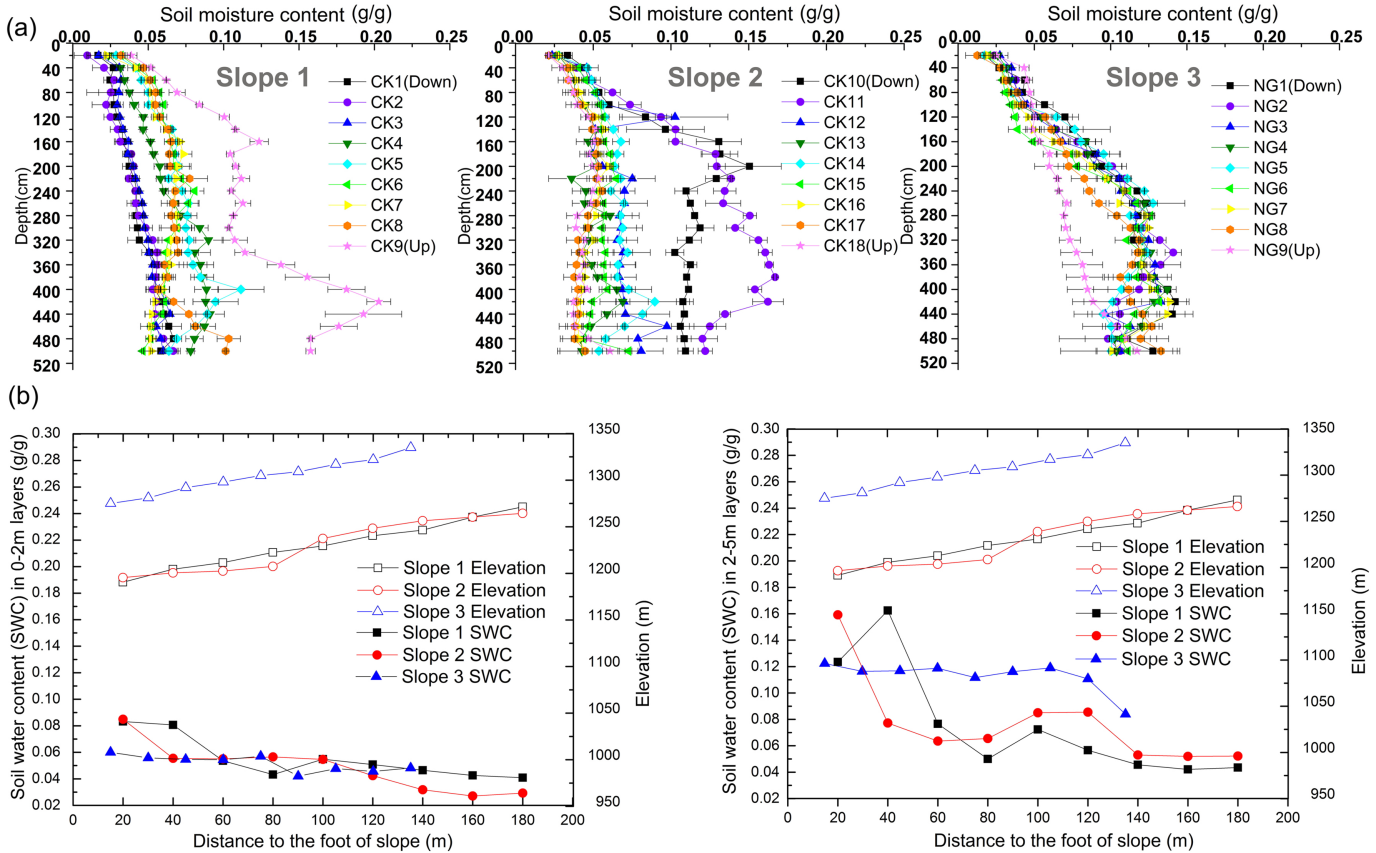
(a)
Soil moisture content (g/g)
Depth(cm)
Slope 1
CK1(Down)
CK2
CK3
CK4
CK5
CK6
CK7
CK8
CK9(Up)
Slope 2
CK10(Down)
CK11
CK12
CK13
CK14
CK15
CK16
CK17
CK18(Up)
Slope 3
NG1(Down)
NG2
NG3
NG4
NG5
NG6
NG7
NG8
NG9(Up)
(b)
Soil water content (SWC) in 0-2m layers (g/g)
Slope 1 Elevation
Slope 2 Elevation
Slope 3 Elevation
Slope 1 SWC
Slope 2 SWC
Slope 3 SWC
Elevation (m)
Distance to the foot of slope (m)
Soil water content (SWC) in 2-5m layers (g/g)

Figure 3

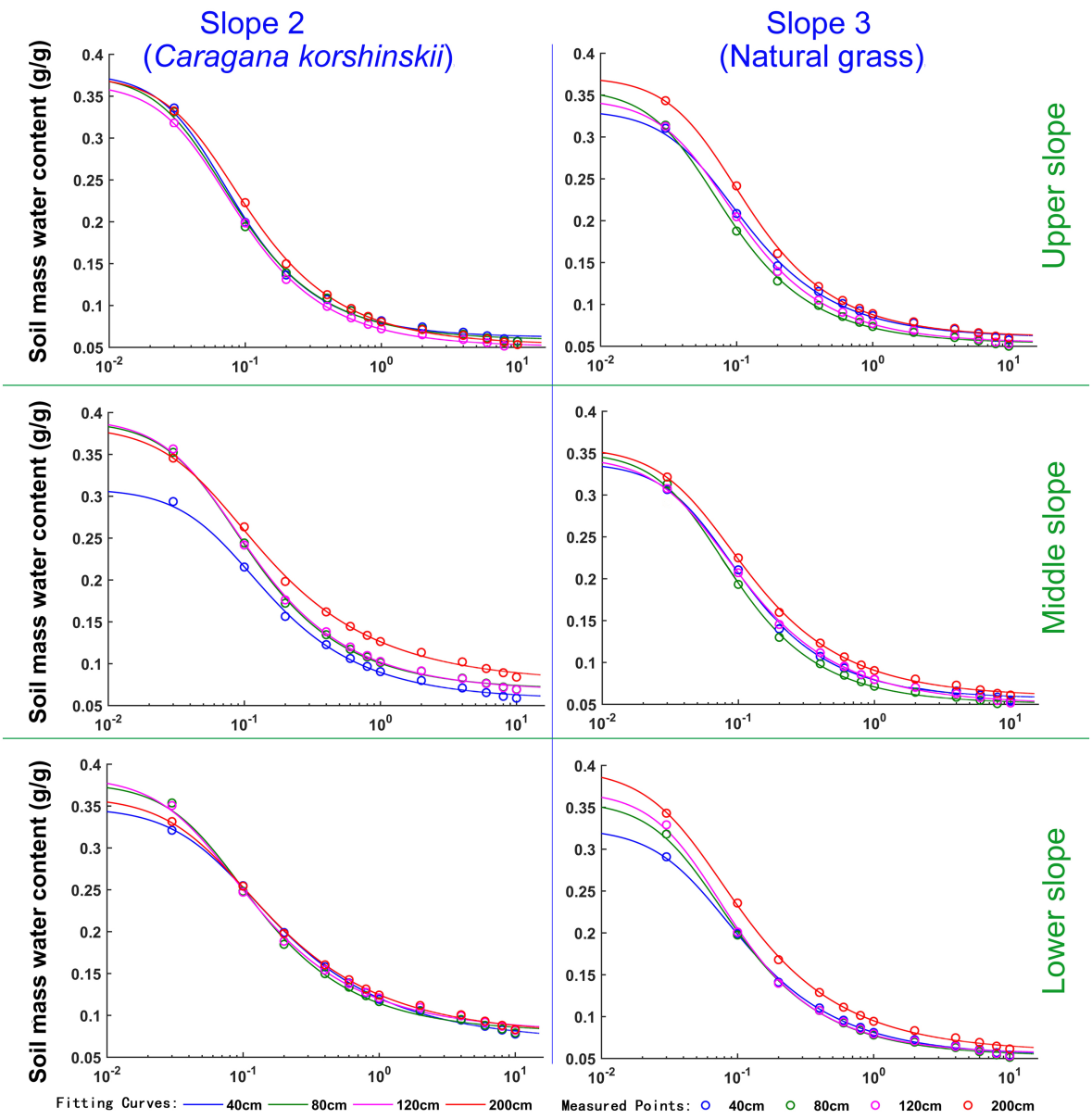
Slope 2
(Caragana korshinskii)
Slope 3
(Natural grass)
Upper slope
Middle slope
Lower slope
Soil mass water content (g/g)
Soil potential energy (100KPa)
Fitting Curves: 40cm 80cm 120cm 200cm
Measured Points: 40cm 80cm 120cm 200cm

Figure 4

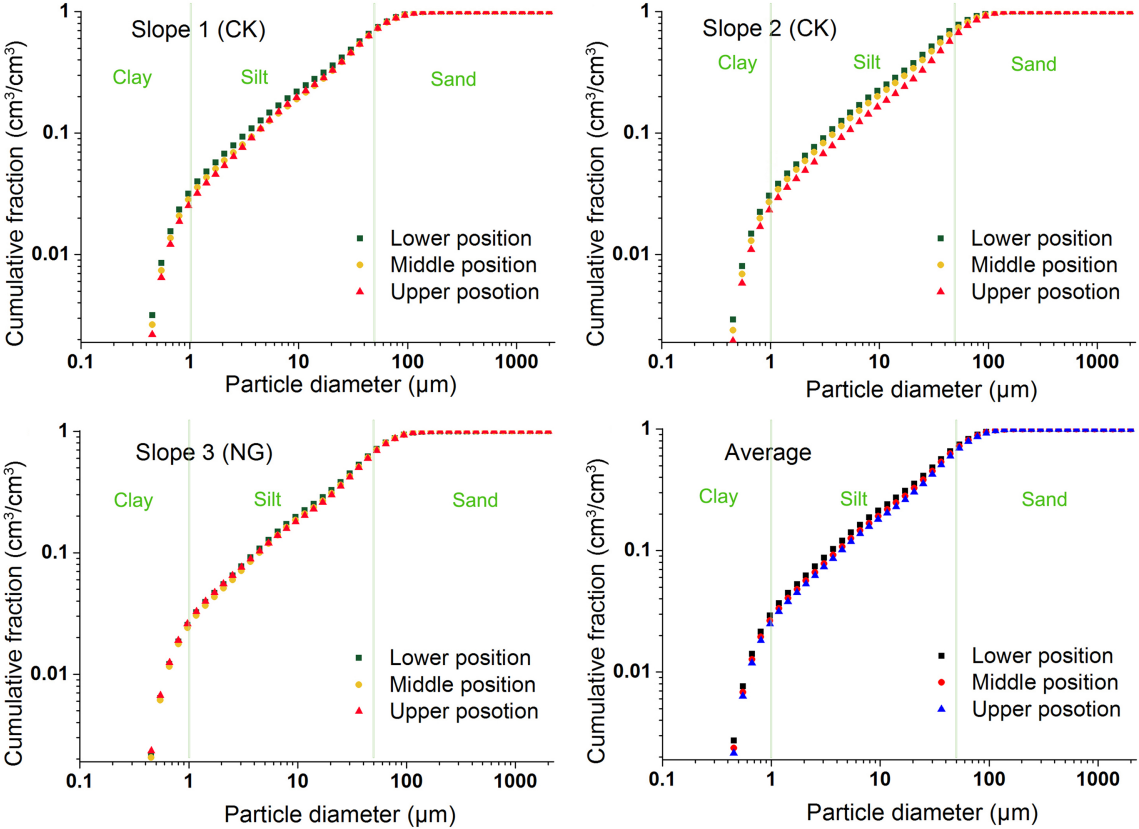
Slope 1 (CK)
Clay
Silt
Sand
Lower position
Middle position
Upper posotion
Cumulative fraction (cm3/cm3)
Particle diameter (μm)
Slope 2 (CK)
Slope 3 (NG)
Average

Figure 5

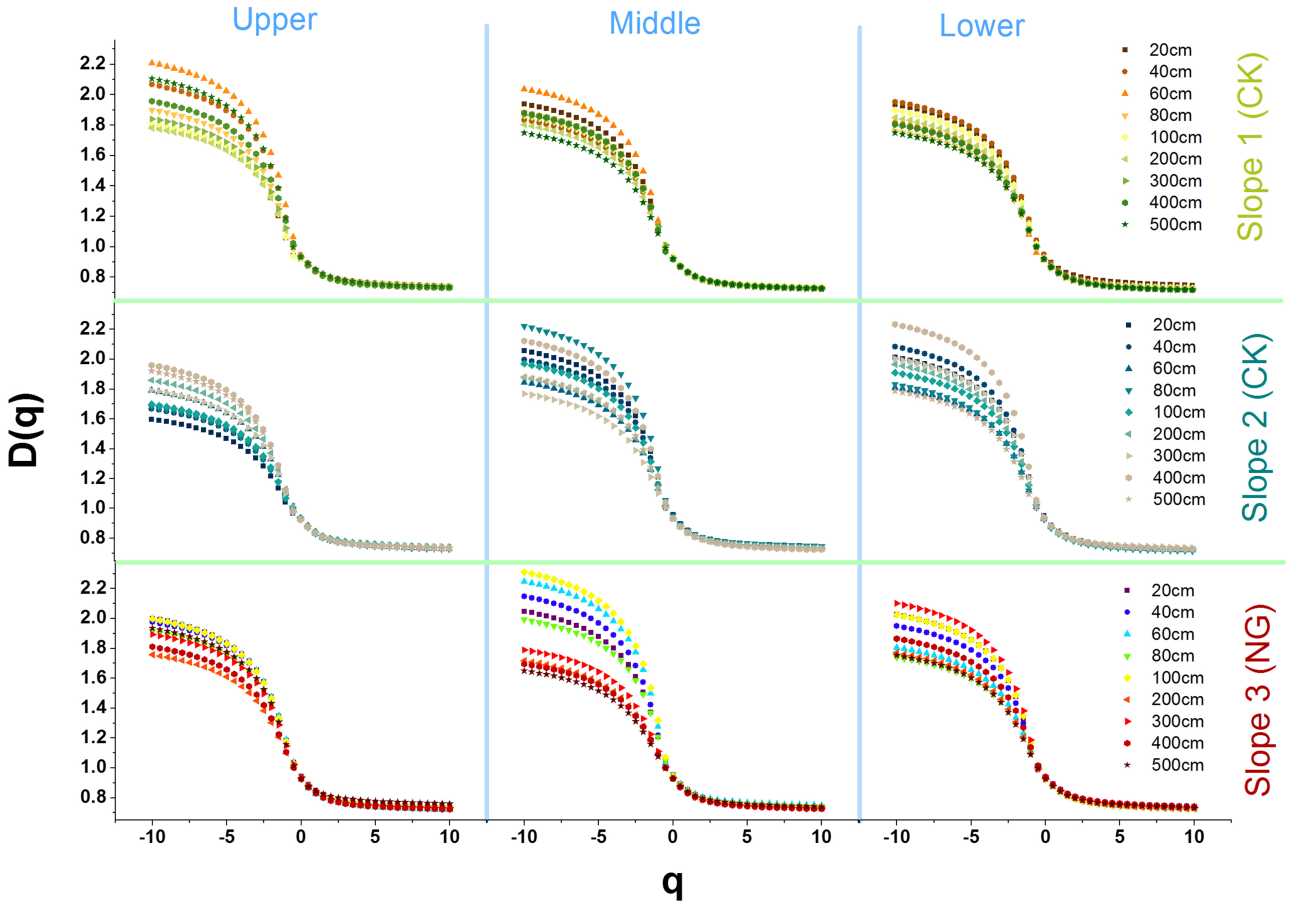
Upper
Middle
Lower
Slope 1 (CK)
Slope 2 (CK)
Slope 3 (NG)
20cm
40cm
60cm
80cm
100cm
200cm
300cm
400cm
500cm
D(q)
q
2.2
2.0
1.8
1.6
1.4
1.2
1.0
0.8
-10
-5
0
5
10

Figure 6

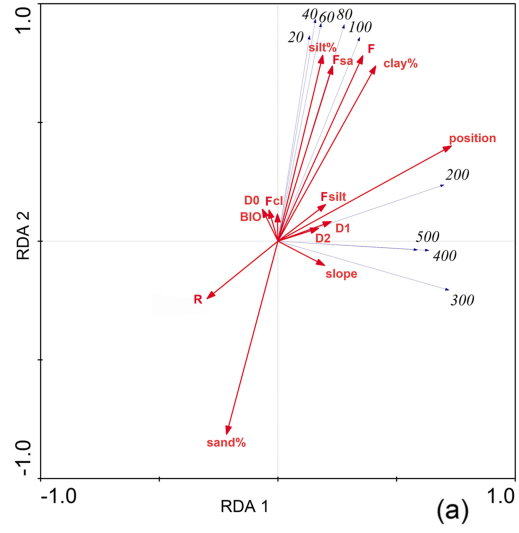
1.0
-1.0
RDA 2
-1.0
RDA 1
1.0
(a)
40
60
80
100
20
silt%
Fsa
F
clay%
position
200
D0
Fcl
BIO
Fsilt
D1
D2
500
400
slope
R
300
sand%

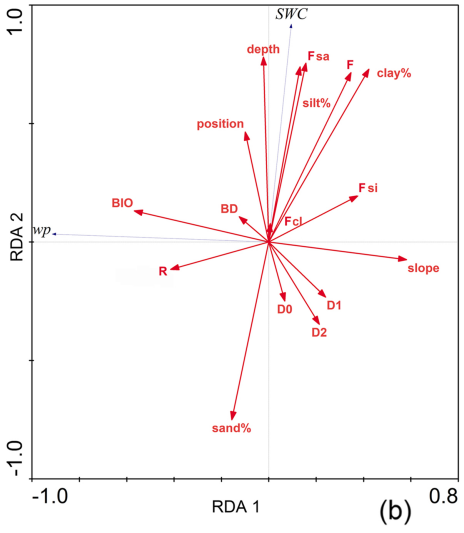
1.0
-1.0
RDA 2
-1.0
RDA 1
0.8
(b)
SWC
depth
Fsa
F
clay%
silt%
position
Fsi
BIO
BD
Fcl
wp
R
slope
D0
D1
D2
sand%

Figure 7